



## 1 **A versatile, refrigerant-free cryofocusing-thermodesorption** 2 **unit for preconcentration of traces gases in air**

3 F. Obersteiner<sup>1</sup>, H. Bönisch<sup>2</sup>, T. Keber<sup>1</sup>, S. O'Doherty<sup>3</sup> and A. Engel<sup>1</sup>

4 <sup>1</sup> Institute for Atmospheric and Environmental Science, Goethe University Frankfurt,  
5 Frankfurt, Germany

6 <sup>2</sup> Institute of Meteorology and Climate Research, KIT, Karlsruhe, Germany

7 <sup>3</sup> School of Chemistry, University of Bristol, Bristol, United Kingdom

8 *Correspondence to:* F. Obersteiner, obersteiner@iau.uni-frankfurt.de

9 **Abstract.** We present a compact and versatile cryofocusing-thermodesorption unit, which we  
10 developed for quantitative analysis of halogenated trace gases in ambient air. Possible appli-  
11 cations include aircraft-based in-situ measurements, in-situ monitoring and laboratory opera-  
12 tion for the preconcentration of analytes from flask samples. Analytes are trapped on adsorp-  
13 tive material cooled by a Stirling cooler to low temperatures (e.g.  $-80\text{ }^{\circ}\text{C}$ ) and desorbed sub-  
14 sequently by rapid heating of the adsorptive material (e.g.  $+200\text{ }^{\circ}\text{C}$ ). The setup neither in-  
15 volves exchange of adsorption tubes nor any further condensation or refocussation steps. No  
16 moving parts are used that would require vacuum insulation. This allows a simple and robust  
17 single-stage design. Reliable operation is ensured by the Stirling cooler, which does not re-  
18 quire refilling of a liquid refrigerant while allowing significantly lower adsorption tempera-  
19 tures compared to commonly used Peltier elements. We use gas chromatography - mass spec-  
20 trometry for separation and detection of the preconcentrated analytes after splitless injection.  
21 A substance boiling point range of approximately  $-80\text{ }^{\circ}\text{C}$  to  $+150\text{ }^{\circ}\text{C}$  and a substance mixing  
22 ratio range of less than 1 ppt ( $\text{pmol mol}^{-1}$ ) to more than 500 ppt in preconcentrated sample  
23 volumes of 0.1 to 10 L of ambient air is covered, depending on the application and its analyti-  
24 cal demands. We present the instrumental design of the preconcentration unit and demonstrate  
25 capabilities and performance through the examination of injection quality, analyte break-  
26 through and analyte residues in blank tests. Application examples are given by the analysis of  
27 flask samples collected at Mace Head Atmospheric Research Station in Ireland using our la-  
28 boratory GC-TOFMS instrument and by data obtained during a research flight with our in-situ  
29 aircraft instrument GhOST-MS.



## 1 1 Introduction

2 Atmospheric trace gases introduced to or elevated in concentration in the environment by hu-  
3 man activities often show adverse environmental impacts. Prominent examples are chloro-  
4 fluorocarbons (CFCs) and their intermediate replacements, hydrochlorofluorocarbons  
5 (HCFCs), which deplete stratospheric ozone (Farman et al., 1985; Molina and Rowland,  
6 1974; Montzka et al., 2011; Solomon, 1999). Present-day CFC-replacements, namely hydro-  
7 fluorocarbons (HFCs), have zero ozone depletion potentials (ODPs) but are still potent green-  
8 house gases like CFCs and HCFCs (Hodnebrog et al., 2013; Velders et al., 2009). Another  
9 example are non-methane hydrocarbons (NMHCs), which produce harmful tropospheric  
10 ozone in the presence of nitrogen oxides (Haagen-Smit and Fox, 1956; Marenco et al., 1994;  
11 Monks et al., 2015).

12 Many of the species found in the compound classes named above show atmospheric concen-  
13 trations too low for direct detection and quantification by means of instrumental analytics.  
14 Therefore, a preconcentration step is required. The method of cryofocusing-thermodesorption  
15 is a common technique for that purpose (e.g. Aragón et al., 2000; Demeestere et al., 2007;  
16 Dettmer and Engewald, 2003; Eyer et al., 2016; Hou et al., 2006). In principal, an ambient air  
17 sample from either a sample flask or continuous flow for online measurement is preconcent-  
18 rated on adsorptive material at a specific adsorption temperature,  $T_A$ . If  $T_A$  is significantly  
19 below ambient temperature, this step is referred to as “cryofocusing” or “cryotrapping”.  
20 Trapped analytes are re-mobilized subsequently by heating the adsorptive material to a de-  
21 sorption temperature  $T_D$  and flushed e.g. onto a gas chromatographic column with a carrier  
22 gas and detected with a suitable detector.

23 The primary motivation for the development of the instrumentation described in this manu-  
24 script was halocarbon analysis in ambient air. More specifically, there were no commercial  
25 instruments available which met the requirements of remote in-situ and aircraft operation:  
26 compact (as small as possible), lightweight (<5 kg), safe containment of working fluids and  
27 preferentially cryogen-free, pure electrical operation. Liquid cooling agents like liquid nitro-  
28 gen ( $LN_2$ ) or argon (LAr) (e.g. Apel et al., 2003; Farwell et al., 1979; Helmig and Greenberg,  
29 1994) offer large cooling capacity but are difficult to operate on board of an aircraft due to  
30 safety restrictions and supply demand, e.g. when operating the aircraft from remote airports.  
31 Compression coolers (e.g. Miller et al., 2008; O'Doherty et al., 1993; Saito et al., 2010) offer  
32 less cooling capacity in terms of heat lift compared to liquid cooling agents and are relatively



1 large in size and weight compared to widespread Peltier type cooling options (Peltier ele-  
2 ments; e.g. de Blas et al., 2011; Simmonds et al., 1995; commercial thermodesorbers available  
3 from e.g. Markes or PerkinElmer). Peltier elements have the advantage of being very small  
4 and requiring only electrical power for cooling. However, their cooling capacity and mini-  
5 mum temperature cannot compete with compression- and refrigerant-based coolers. Stirling  
6 coolers pose an in-between solution, well-suited for maintenance-free remote operation: like  
7 Peltier coolers, they only require electrical power, do not contain any potentially dangerous  
8 working fluids (only helium) or cryogenics but have a significantly higher cooling capacity.  
9 While not being as powerful as refrigerant-based coolers (LN<sub>2</sub>, LAr), they still have compara-  
10 ble minimum temperatures. To our knowledge, the use of Stirling coolers for similar purposes  
11 like the one described here is rare with few published exceptions like the preconcentration of  
12 methane by Eyer et al. (2016) or the trapping of CO<sub>2</sub> as a carbon capture technology by Song  
13 et al. (2012).

14 The principal design of the cryofocusing-thermodesorption unit in description was developed  
15 for the airborne in-situ instrument GhOST-MS (Gas chromatograph for the Observation of  
16 Tracers – coupled with a Mass Spectrometer, Sala et al., 2014) and successfully used during  
17 three research campaigns up to now – 2011: SHIVA (carrier aircraft: DLR FALCON), 2013:  
18 TACTS (carrier aircraft: DLR HALO), 2015/2016: PGS (carrier aircraft: DLR HALO). To  
19 extend the substance range, we then developed similar cryofocusing-thermodesorption units  
20 for our other GC-MS instruments (Hoker et al., 2015; Obersteiner et al., 2016), which are  
21 currently operated in the laboratory. Both detailed description and characterisation of the pre-  
22 concentration unit were not discussed in the publications Hoker et al. (2015), Obersteiner et  
23 al. (2016) (laboratory setups) and Sala et al. (2014) (aircraft instrument). Within this manu-  
24 script, a general instrumental description is given in section 2, which is applicable for all the  
25 named setups. Characterisation results discussed in section 3 are based on the latest version of  
26 the laboratory setup (Obersteiner et al., 2016). To demonstrate the versatility and reliability of  
27 the setup, application examples are given in section 4 for sample analysis in the laboratory as  
28 well as in-situ aircraft operation. Results are summarized and conclusions are drawn in sec-  
29 tion 5.



## 1    **2 Instrumentation**

2    This section gives a description of principal components of the sample preconcentration unit  
3    and is valid for all our analytical setups presented in Sala et al. (2014), Hoker et al. (2015) and  
4    Obersteiner et al. (2016). The following section 2.1 outlines the general measurement proce-  
5    dure and gas flow as well as its integration into a chromatographic detection system. Sections  
6    2.2 and 2.3 describe the implementation of the main operations of the unit; cooling (“trap-  
7    ping”, i.e. preconcentration of analytes) and heating (desorption of analytes). A preconcentra-  
8    tion system can always only be as good as the analytical set-up behind it. The pre-  
9    concentration system described here has been designed for the coupling with a chromato-  
10   graphic system but in principle could also be adapted for coupling with other techniques. Spe-  
11   cific technical components of the instrumentation used in this work to characterise the pre-  
12   concentration unit will be listed in section 3.

### 13    **2.1 Measurement procedure and gas flow in GC application**

14   For the preconcentration of analytes, the sample is flushed through a micro packed column of  
15   cooled adsorptive material. Analytes are “trapped” on the adsorptive material as the steady  
16   state of adsorption and desorption is strongly shifted towards adsorption by the low tempera-  
17   ture of the adsorptive material. By subsequent rapid heating of the adsorptive material, the  
18   steady state is instantaneously shifted towards desorption (“thermodesorption”). Formerly  
19   trapped analytes are flushed backwards onto the warm chromatographic column with a carrier  
20   gas. There is no further refocusing or separation step, except for higher-boiling compounds on  
21   the GC column itself. **Figure 1** shows a flow scheme of the setup. The outflow of the sample  
22   loop during preconcentration (“stripped air”; mainly nitrogen and oxygen) is collected in a  
23   previously evacuated reference volume for analyte quantification (2 L electro-polished stain-  
24   less steel flask; volume determination by pressure difference). A mass flow controller (MFC)  
25   is mounted between sample loop and reference volume for sample flow control. The MFC can  
26   also be used for sample volume determination e.g. for sample volumes larger than the refer-  
27   ence volume. Hardware control is implemented with a LabVIEW cRIO assembly (compact,  
28   reconfigurable input output; National Instruments Inc., USA) using self-written control soft-  
29   ware. It operates the preconcentration unit automatically, i.e. controls system parameters like  
30   sample loop temperature by cooling and heating concomitant with system states like precon-  
31   centration, desorption etc.



## 1 2.2 Cryofocusing: sample loop and cooling technique

2 A stainless steel tube with 1/16" outer diameter (OD) and 1 mm inner diameter (ID) is used as  
3 sample loop. The tube is packed with adsorptive material and placed inside an aluminium  
4 cuboid ("coldhead") which is cooled continuously to maintain a specific adsorption tempera-  
5 ture. **Figure 2** shows a technical drawing of sample loop and coldhead. The coldhead can con-  
6 tain two sample loops; in this case one of them is an empty stainless steel tube with 1/16 inch  
7 OD and 1 mm ID to characterize the sample loop heater. For that purpose, a thin temperature  
8 sensor is inserted into the empty tube. To save space and avoid mechanical, moving parts, the  
9 sample loop is not removed from the coldhead during desorption. It is insulated and thereby  
10 isolated electrically by two layers of glass silk and four layers of Teflon shrinking hose. The  
11 insulation is a variable parameter which determines the rate at which heat is exchanged be-  
12 tween sample loop and coldhead. Consequently, it determines coldhead warm-up rate during  
13 desorption and sample loop cool-down rate after desorption. More insulation would result in  
14 longer cool-down time after desorption but also to less heat flowing into the cold head, thus to  
15 lower possible temperature of the cold head. The insulation used represents a compromise that  
16 works well for the application presented here but could potentially be improved by e.g. using  
17 a ceramic insulator. The coldhead itself is insulated towards surrounding air with 45 mm of  
18 Aeroflex HF material (Aeroflex Europe GmbH, Germany).

19 The Stirling cooler used for cooling offers the advantage of requiring only electrical power  
20 while providing a relatively large cooling capacity at very low minimum temperatures. The  
21 latter are comparable to liquid nitrogen in case of Sunpower CryoTel MT, CT and GT Stirling  
22 coolers, with maximum heat lifts of 5 W to 16 W at  $-196\text{ }^{\circ}\text{C}$  according to the manufacturer.  
23 Heat that is removed from the coldhead by the Stirling cooler has to be released to the sur-  
24 rounding air; either directly by an air-fin heat rejection or indirectly by a water coolant system  
25 mounted to the cooler's warm side. The cooler should maintain a defined adsorption tempera-  
26 ture  $T_A$  of the sample loop over the series of measurements. However, during thermodesorp-  
27 tion, a certain amount of heat is transferred to the coldhead as the sample loop is kept directly  
28 inside with only a small amount of insulation. Excess heat has to be removed by the Stirling  
29 cooler to regain  $T_A$  for the preconcentration of the next sample. The preconcentration unit is  
30 attached to a gas chromatograph; therefore, the gas chromatographic runtime allows coldhead  
31 and sample loop to cool down after thermodesorption and return to  $T_A$  before preconcentrat-  
32 ing the next sample.



1 Besides chromatographic runtime, various factors determine the minimum cycle time (i.e.  
2 sample measurement frequency) including:

- targeted adsorption temperature  $T_A$
- Stirling cooler's cooling capacity (i.e. heat lift around  $T_A$ ) and coldhead insulation as well as ambient temperature
- thermodesorption duration and  $T_D$  as well as insulation of the sample loop
- volume of the sample to preconcentrate and preconcentration flow

3 To give a practical example, **Table 1** shows cycle times derived from routine operation data.  
4 With the laboratory setup, a total time per measurement of 18.6 minutes is necessary if  
5  $T_A = -120$  °C and  $T_D \approx 200$  °C is desired – mainly determined by the time needed to compen-  
6 sate the warm-up of the coldhead during desorption. This minimum time interval significantly  
7 shortens to 8.5 minutes if  $T_A$  is increased to  $-80$  °C (same  $T_D$ ). Data from the in-situ setup  
8 shown in **Table 1** demonstrates that even shorter cycle times of 4.1 minutes are possible with  
9 a decreased preconcentration volume (100 mL instead of 500 mL; requiring a detector that is  
10 sensitive enough) and a slightly higher  $T_A$ . General measures to increase the number of meas-  
11 urements per time would be to increase the preconcentration flow, reduce the sample size (see  
12 in-situ setup), improve the coldhead and sample loop insulation and increase the cooling ca-  
13 pacity.

14 After desorption, sample loop temperature drops in an exponential decay shaped curve due to  
15 the decreasing temperature difference between coldhead and sample loop. After a desorption  
16 at  $T_D \approx 200$  °C, sample loop and coldhead temperature reached similar temperatures after ap-  
17 proximately 30 s cool-down time ( $T_A = -80$  °C). The cool-down time increases to about 90 s  
18 at  $-120$  °C cold head temperature. Considering the total run times shown in (**Table 1**), sample  
19 loop cool-down time is not a limiting factor to the overall cycle time. Consequently, thermal  
20 insulation of the sample loop could still be increased, thereby decreasing coldhead warm-up  
21 during desorption.



### 1 2.3 Thermodesorption: sample loop heater

2 Depending on the targeted substance class to analyse and the analytical technique, the re-  
3 quirements for thermodesorption will differ. In case of a gas chromatographic system for  
4 analysis of volatile compounds, these requirements are:

- 5 • a fast initial increase in temperature to yield a sharp injection of highly volatile  
6 analytes onto the GC column,
- 7 • no overshooting of a maximum temperature in case of thermally unstable sample  
8 compounds or adsorptive material (e.g. HayeSep D,  $T_D < 290$  °C)
- 9 • preservation of the desorption temperature over a time period for desorption of  
10 analytes with higher boiling points
- 11 • good overall repeatability, especially of the injection of highly volatile analytes

12 Desorption heating is implemented by pulsing a direct current (max. 12 V / 40 A, relay:  
13 Celduk Okpac; spec. switching frequency 1 kHz, Celduk Relays, France) directly through the  
14 sample loop tubing which has a resistance of  $\sim 0.5$   $\Omega$ . A temperature sensor (Pt100, 1.5 mm  
15 OD) was welded to the outside of the sample loop tubing (see also **Figure 2**), for feedback  
16 control of the heater temperature. However, mainly due to the thermal mass of the sensor and  
17 its proximity to the coldhead (despite the insulation), it was found to give no representative  
18 values for temperature inside the sample loop during desorption. Differences of around  
19 100 °C were found in comparison to temperature measured within the sample loop (equilibr-  
20 ium state; after 2-3 minutes of continuous heating). Nevertheless, the temperature sensor can  
21 be (after being characterised) used for feedback control as the indicated values are reproduc-  
22 ible. As an alternative to feedback control, a deterministic heater with prescribed output set-  
23 tings can be used. For security reason, measured coldhead and sample loop temperature have  
24 to be used as heater shutdown triggers in this case.

25 **Figure 3** shows a comparison of temperature sensor data from in- and outside the empty sam-  
26 ple loop as well as the coldhead. Very good results were achieved with a two-stage, determin-  
27 istic heater setup with a fast heat-up, a small overshoot between stage 1 and 2 of the heating  
28 phase and preservation of  $T_D$  with only a small drift and fluctuation. With the described heater  
29 setup,  $T_D$  can be reached within a very short time of approximately 3 seconds. Initial heating  
30 rates (first second of heat pulse) were calculated to be more than 200 °C s<sup>-1</sup> depending on the  
31 power output setting. As the sample loop is getting warmer, heating rate drops resulting in a  
32 mean heating rate of about 80 °C s<sup>-1</sup> during stage 1.



1 If a deterministic heater is used instead of a feedback controlled heater, sample loop tempera-  
2 ture becomes directly dependent on coldhead temperature (more precisely: heat flow from the  
3 sample loop into the coldhead). Consequently, higher output settings are necessary at lower  
4 coldhead temperatures to achieve comparable temperatures. On the other hand, if the cold-  
5 head gets warmer, sample loop temperature increases as well. This effect can be observed in  
6 **Figure 3** as a slight upward drift of the sample loop temperature (red curve, temperature  
7 measured within the sample loop) during stage 2. The absolute temperature differences caused  
8 by this drift as well as the oscillation amplitude are small (approximately 20 °C min. to max.  
9 and 4 °C standard deviation without trend correction) compared to the temperature difference  
10 between coldhead and sample loop during heating (about 300 °C).

11 Besides the problem of differing inner and outer temperature of the sample loop during heat-  
12 ing, temperature was not found to be distributed homogeneously alongside the empty sample  
13 loop inside the coldhead. Temperature differences of up to  $\pm 30$  °C at 200 °C mean tempera-  
14 ture were observed with the current setup if measuring temperature at different points within  
15 the sample loop, potentially due to (a) difficulties in accurately measuring the inner tempera-  
16 ture (wall contact of sensor) and (b) inhomogeneity in sample loop insulation as well as varia-  
17 tions in tubing wall width or carbon content leading to an inhomogeneous electrical resistance  
18 and thus an inhomogeneous distribution of heat. These temperature variations might be differ-  
19 ent or ideally negligible in the sample loop packed with adsorptive material. However, the  
20 finding underlines the importance of an insulation as homogeneous as possible and suggests  
21 that “cold points” (possibility of insufficient desorption) as well as “hot points” (possibility of  
22 adsorptive material or analyte decomposition) are possible along the sample loop, which has  
23 to be taken into consideration when setting up and testing the preconcentration setup, i.e. to  
24 not exceed the temperature limit of the adsorptive material.





### 1 **3 Characterisation**

2 This section discusses characterisation results (section 3.2 and 3.3) obtained with the  
3 GC-TOFMS instrument described in Obersteiner et al. (2016) as it covers the widest sub-  
4 stances range (see supplementary information) and therefore allows the most differentiated  
5 analysis. A brief description of this analytical instrument is given in the following section 3.1;  
6 see Obersteiner et al. (2016) for details on GC and MS. We consider these results to be valid  
7 in principle also for our other GC-MS setup discussed by Hoker et al. (2015) and the GhOST-  
8 MS described by Sala et al. (2014) as all preconcentration setups rely on the same principal  
9 setup and similar components are used.

#### 10 **3.1 Analytical instrument**

11 A Sunpower CryoTel CT free piston Stirling cooler (Ametek Inc., USA) is used for cooling of  
12 the coldhead. In the described setup, a water coolant system (Alphacool, Germany) originally  
13 intended for cooling of a personal computer's processing units removes heat from the Stirling  
14 cooler's heat rejection. Sunpower Stirling coolers are optionally also available with an air-fin  
15 heat rejection that requires a continuous air stream during operation. For sample loop heater  
16 control, a pulse-width modulation (PWM; 20 ms period, 1  $\mu$ s minimum width) with a pre-  
17 scribed output is used (deterministic heater; see section 2.3). Heater operation during desorp-  
18 tion is separated into a short initial "heat-up" stage with a high output of the PWM and a  
19 longer "hold" stage with lower heater output to maintain desorption temperature. The sample  
20 loop is packed with adsorptive material over a length of approximately 100 mm (~20 mg).  
21 Two different adsorptive materials were used in different sample loops installed in the course  
22 of this work; HayeSep D, 80/100 mesh (VICI International AG, Switzerland) and  
23 Unibeads 1S, 60/80 mesh (Grace, USA).

24 A Bronkhorst EL-FLOW F-201CM (Bronkhorst, the Netherlands) is used for sample flow  
25 control (downstream of the sample loop in order to avoid contamination) in combination with  
26 a Baratron 626 pressure sensor (0-1000 mbar, accuracy incl. non-linearity 0.25 % of reading,  
27 MKS Instruments, Germany) for analyte quantification by pressure difference measurement.  
28 An Agilent 7890 B gas chromatograph (GC) with a GS GasPro PLOT column (Agilent Tech-  
29 nologies, Inc. USA; 0.32 mm inner diameter) using a ramped temperature program (45 °C to  
30 200 °C with 25 °C min<sup>-1</sup>) and backflush option is used for analyte separation. Purified helium  
31 6.0 is used as carrier gas (Praxair Technologies Inc., German supplier; purification system:



1 Vici Valco HP2). For analyte detection, a Tofwerk EI-TOF (model EI-003, Tofwerk AG,  
2 Switzerland) mass spectrometer (MS) is attached to the GC. All samples are dried using mag-  
3 nesium perchlorate kept at 80 °C prior to preconcentration. Artificial additions of analytes to  
4 the sample from the dryer were excluded by comparing measurements of dried and undried  
5 blank gas. All tubing upstream of the sample loop was heated to >100 °C to avoid substance  
6 loss to tubing walls.

7 **Figure 4** shows a typical chromatogram from an ambient air sample for three selected  
8 mass-to-charge ratios (m/Q). Two different adsorptive materials were used in the course of  
9 this work (HayeSep D, Unibeads 1S) which showed partly differing adsorption and desorption  
10 properties; results are discussed separately if appropriate. To achieve high measurement pre-  
11 cision and minimum uncertainties introduced by the preconcentration unit, both the analyte  
12 adsorption (preconcentration) and analyte desorption (injection) into the chromatographic  
13 system have to be quantitative and repeatable. The following section describes tests and re-  
14 sults for the characterisation of both aspects.

### 15 **3.2 Adsorption**

16 The sample loop essentially is a micro packed chromatographic column with a limited surface  
17 area where sorption can take place. The low temperature during sample preconcentration  
18 shifts the steady state of analyte partitioning between mobile and solid phase mostly to the  
19 solid phase. This preconcentration technique “strips” the air of its most abundant constituents;  
20 nitrogen, oxygen and argon. Other, less volatile but still very abundant constituents like CO<sub>2</sub>  
21 are however trapped, depending on adsorption temperature. Elution of such species from the  
22 GC column after thermodesorption and injection can cause problems with regard to chroma-  
23 tography as well as detection, depending on GC configuration and detection technique. With  
24 the setup described here, the elution of CO<sub>2</sub> limits the analysable substance range as the detec-  
25 tor shows saturation during the elution of CO<sub>2</sub>. Regarding preconcentration of targeted ana-  
26 lytes, the concept of an adsorption-desorption steady state suggests that at a certain point a  
27 breakthrough of analytes occurs, depending on a combination of loading of the solid phase  
28 with sample molecules and time to achieve steady state, in turn influenced by sample flow  
29 rate and pressure. Consequently, the maximum possible sample volume and/or minimum du-  
30 ration of preconcentration are dependent on the adsorptive material used, volatility (and con-  
31 centration) of the targeted analytes as well as sample flow rate and pressure. For typical sam-  
32 ple volumes of 0.5 L and 1.0 L (at standard temperature and pressure) and a constant sample



1 back pressure of 2.5 bar abs., no significant impact of sample preconcentration flow was  
2 found within the tested range of  $50 \text{ mL}\cdot\text{min}^{-1}$  to  $150 \text{ mL}\cdot\text{min}^{-1}$  for any of the analysed sub-  
3 stances. Higher or lower flow rates and pressure were not possible or suitable for practical  
4 reasons like flow restriction and valve operating pressure.

5 Substance breakthrough (i.e. substance-specific adsorption capacity) was analysed in volume  
6 variation experiments, comprising measurements of the same reference air with preconcentra-  
7 tion volumes of up to 10 L and referencing the volume-corrected detector response against  
8 default preconcentration volumes of e.g. 1 L (“relative response”). Quantitative trapping is  
9 then indicated by a relative response of 1; a relative response  $<1$  would indicate an underesti-  
10 mation (i.e. loss by breakthrough), a relative response of  $>1$  would indicate an overestimation  
11 (i.e. increase by a memory effect from the preceding sample). To structure the following dis-  
12 cussion, two classes of substances are formed and treated separately: “medium volatile sub-  
13 stances” with boiling points  $> -30 \text{ }^\circ\text{C}$  (e.g. CFC-12,  $\text{CCl}_2\text{F}_2$ ) and “highly volatile substances”  
14 with boiling points  $< -30 \text{ }^\circ\text{C}$  (e.g. HFC-23,  $\text{CHF}_3$ ). The substances discussed are selected  
15 based on the criteria volatility and (preferably high) concentration. The adsorption of sub-  
16 stances with lower volatility (BP  $> 30 \text{ }^\circ\text{C}$ ) was assumed to be quantitative. Results discussed  
17 in the following are displayed in **Table 2**.

18 **Medium volatile substances.** As a reference for halocarbon analysis, CFC-12 ( $\text{CCl}_2\text{F}_2$ ) and  
19 CFC-11 ( $\text{CCl}_3\text{F}$ ) were chosen due to their high mixing ratios of about 525 and  
20  $235 \text{ pmol}\cdot\text{mol}^{-1}$  (ppt, parts per trillion) in present-day, ambient air and moderate volatility  
21 with boiling points of  $-29.8 \text{ }^\circ\text{C}$  and  $+23.8 \text{ }^\circ\text{C}$ . For a volume of 10 L preconcentrated air on the  
22 Unibeads 1S sample loop, both substances showed a deviation from linear response of  
23  $+0.6 \% \pm 0.42 \%$  for CFC-12 and  $+0.6 \% \pm 0.22 \%$  respectively for CFC-11. The positive  
24 deviation from linearity is still found within the 3-fold measurement precision determined for  
25 the experiment and could potentially be an artefact of the detector used which tends to slightly  
26 overestimate strong signals and underestimate weak signals; see section 3.4 in  
27 Obersteiner et al. (2016). Hence, no significant breakthrough or detector saturation was ob-  
28 served for both substances CFC-12 and CFC-11.

29 **Highly volatile substances.** More volatile compared to CFC-12 and CFC-11 but similar in  
30 mixing ratio is carbonyl sulfide (COS) with a boiling point of  $-50.2 \text{ }^\circ\text{C}$  and an ambient air  
31 mixing ratio of typically around 500 ppt. Against 1 L reference sample volume (sample  
32 mixing ratio: 525 ppt), COS showed a quantitative adsorption up to 5 L on the Unibeads 1S



1 sample loop with a deviation from linear response of  $+0.9 \% \pm 0.80 \%$ . At 10 L sample  
2 volume, a breakthrough occurred giving a deviation from linear response of  
3  $-35.2 \% \pm 0.52 \%$ . The substance analysed with highest volatility was HFC-23 with a boiling  
4 point of  $-82.1 \text{ }^\circ\text{C}$  and a current background air mixing ratio of  $\sim 40$  ppt. Referenced against a  
5 sample volume of 0.5 L, significant breakthrough occurred at a sample volume of 2.5 L with a  
6 deviation from linear response of  $-39.2 \% \pm 2.75 \%$ . The highest sample volume quantitative-  
7 ly adsorbed in the experiment was 1.0 L with a relative response of  $-0.3 \% \pm 2.75 \%$   
8 (HayeSep D sample loop). A similar behaviour was observed for ethyne ( $\text{C}_2\text{H}_2$ ), with a subli-  
9 mation point of  $-80.2 \text{ }^\circ\text{C}$ , a mixing ratio of approximately 610 ppt in the sample and a devia-  
10 tion from linear response of  $-20.2 \% \pm 1.22 \%$  at 2.5 L sample volume (HayeSep D sample  
11 loop). However, ethyne was also analysed on the Unibeads 1S sample loop which gave a quite  
12 different result with a deviation from linear response of  $+10.1 \% \pm 0.51 \%$ , thus breakthrough  
13 did not occur. The positive, non-linear response is caused potentially by a system blank (see  
14 also section 3.3). Unfortunately, HFC-23 could not be analysed in ambient air samples for  
15 comparison on the Unibeads 1S sample loop as its ion signals are masked by large amounts of  
16  $\text{CO}_2$  still eluting from the GC column at the retention time of HFC-23.

17 Concluding, the adsorption process was found to be substance specific as both HFC-23 and  
18 ethyne are comparably volatile but significantly less ethyne broke through despite its 15-fold  
19 elevated mixing ratio (Unibeads 1S sample loop). The comparison of ethyne breakthrough on  
20 the HayeSep D and Unibeads 1S sample loop suggests that the adsorption process is depend-  
21 ent on the chosen adsorptive material. A comparison of adsorptive materials is however not  
22 the focus of this work; such a comparative adsorption study was e.g. conducted for methane  
23 ( $\text{CH}_4$ ) preconcentration by Eyer et al. (2014). From the comparison of the breakthrough ob-  
24 served for COS and the quantitative adsorption of CFC-12 and CFC-11, it can be concluded  
25 that volatility is the primary factor that determines breakthrough. Quantitative adsorption is  
26 not limited by principal adsorption capacity (i.e. the absolute number of molecules adsorbed)  
27 of the adsorptive material and material amount for a sample volume of up to 10 L and an ad-  
28 sorption temperature of  $-80 \text{ }^\circ\text{C}$ .

29



### 1 3.3 Desorption

2 While adsorption is characterised by the quantitative trapping of highly volatile substances,  
3 desorption is characterised by sharpness and repeatability of the injection represented by  
4 chromatographic peak shape and retention time variance (qualitative aspect; section 3.3.1) as  
5 well as the amount of blank residues (quantitative aspect; section 3.3.2). Blank residues  
6 (“memory effect”) have to be divided into residues that remain on the adsorptive material  
7 after desorption (“preconcentration residues” or “preconcentration memory effect”) and resi-  
8 dues that remain in the analytical setup (tubing etc.) upstream of the sample loop, thus had not  
9 reached the sample loop (“system residues” or “system memory effect”).

#### 10 3.3.1 Peak shape and retention time stability

11 To demonstrate injection sharpness, **Figure 5 A** shows the chromatographic signal of CFC-11  
12 eluted from the GC column kept isothermal at 150 °C and **Figure 5 B** the chromatographic  
13 signal as observed with the ramped GC program. Both signals generally show a Gaussian  
14 peak shape with a slight tailing of the right flank. In comparison, the “unfocused” signal from  
15 the isothermal column reflecting the sharpness of the direct injection is wider by a factor of  
16 ~3 but still narrow enough to allow for good peak separation in most standard GC methods  
17 with runtimes between 10 to 30 minutes; the full peak width at half maximum (FWHM) was  
18 calculated to be 6.3 s (0.10 min) for the isothermal peak and 2.0 s (0.03 min) for the focused  
19 peak.

20 Injection quality can further be judged by the stability of retention times of the first chromato-  
21 graphic signals obtained with the ramped GC program, as these are only very little influenced  
22 by the chromatographic system (in particular there is nearly no refocusing on the chromato-  
23 graphic column). **Table 3** shows retention times and their variability expressed as relative  
24 standard deviation and variance as well as the chromatographic signal width (FWHM) of the  
25 respective substance. Variances are less than 0.02 s on average. Together with signal width,  
26 they decrease reversely proportional to retention time, which shows the increasing influence  
27 of chromatographic separation (from HFC-23 to CFC-11 in **Table 3**). Even at incomplete re-  
28 focusation by gas chromatography, the desorption procedure of the preconcentration unit  
29 gives close to Gaussian peak shapes except a slight tailing of the right flank. The tailing effect  
30 could potentially be reduced by refocusing the high-volatile analyte fraction on a second sam-  
31 ple loop. The high repeatability of the injection is shown by the low variability in retention  
32 time of the first signals in the chromatogram (**Table 3**).



### 1 **3.3.2 Analyte residues**

2 Analyte residues can originate from inherent system *contamination* or constitute a remainder  
3 from the previous sample (*memory effect*). Analyte residues were investigated with (a) an  
4 unloaded injection after multiple 1 L ambient air sample injections, i.e. subsequent thermode-  
5 sorption of the sample loop without switching to load-position between runs (see **Figure 1**)  
6 and (b) the preconcentration of 1 L helium from the carrier gas supply using the same path as  
7 the sample, including dryer etc. after multiple 1 L ambient air sample measurements. Analyte  
8 residues on the sample loop (*sample loop memory*) as well as carrier gas contaminations are  
9 investigated by (a) while (b) includes analyte residues within the tubing upstream of the sam-  
10 ple loop, i.e. stream selection, sample dryer etc. (*system memory*). To get the most complete  
11 picture possible, 65 substances were analysed, most of them halo- and hydrocarbons (see sup-  
12 plementary information for a detailed list) on both a HayeSep D as well as a Unibeads 1S  
13 sample loop. Substances with low measurement precision ( $> 10\%$ ) were excluded from the  
14 investigation.

15 In general, most of the detected analyte residues are most probably caused by system contam-  
16 inations (HFCs from fittings, solenoid valve membranes etc.) or carrier gas contaminations  
17 (hydrocarbons) as they show a constant background. In principal, the amount of a residue is  
18 dependent on volatility and concentration, so extremely elevated concentrations of low-  
19 volatile substances might lead to a memory effect that was not detected in the current investi-  
20 gation with 1 L preconcentration volume of unpolluted ambient air. Detailed results for the  
21 two different adsorptive materials tested are discussed in the following.

22 **Unibeads 1S adsorptive material.** 13 of 65 substances (20 %) did show detectable residues on  
23 the sample loop which did not represent a system memory but a system contamination, e.g.  
24 from the carrier gas, sealing materials etc. as they were always present and did not disappear  
25 in subsequent unloaded injections. Respective residues were generally larger with increasing  
26 boiling point (e.g. n-propane  $<$  benzene). Most of them were hydrocarbons and the halocar-  
27 bons chloro- and iodomethane ( $\text{CH}_3\text{Cl}$ ,  $\text{CH}_3\text{I}$ ) and chloroethane ( $\text{C}_2\text{H}_5\text{Cl}$ ) as well as HFC-134  
28 ( $\text{CHF}_2\text{CHF}_2$ ). No further CFCs, HCFCs, PFCs or HFCs were detected in the unloaded sample  
29 loop injection (see Obersteiner et al. (2016) for a discussion of detection limits). Of the re-  
30 maining 52 substances, 36 also did not show any detectable residues in the helium blank. Of  
31 the 17 substances that did show residues (contamination and memory effect combined), 7 had  
32 residues below 0.5 % of the signal area determined in the preceding ambient air measurement.  
33 Again, residues were found mostly for hydrocarbons but not CFCs or HCFCs. Concluding,



1 the Unibeads 1S sample loop seems to be a good choice for halocarbon monitoring measure-  
2 ments (one measurement per sample) as there were nearly no halocarbon residues in subse-  
3 quent helium blank measurements.

4 ***HayeSep D adsorptive material.*** The HayeSep D sample loop showed a considerably higher  
5 amount of sample loop residues with 22 detectable substances from the selected 65 (34 %).  
6 Again, most of these substances were hydrocarbons but also some halogenated compounds  
7 like Tetrachloromethane ( $\text{CCl}_4$ ) and Bromoform ( $\text{CHBr}_3$ ). Of the remaining 43 substances, 28  
8 were undetectable in the helium blank (system free of contamination and memory effect). 13  
9 of the detectable substances showed responses of  $< 0.5$  % relative to the preceding ambient air  
10 sample, also including CFC-11 with 0.05 % and CFC-113 with 0.2 %. While the named halo-  
11 genated compounds  $\text{CCl}_4$  and  $\text{CHBr}_3$  as well as CFC-113 and CFC-11 were undetectable in  
12 subsequent blank gas measurements, residues of many hydrocarbons were persistent, suggest-  
13 ing a system contamination. In summary, the HayeSep D sample loop showed an overall  
14 higher number of residues which is likely caused by a higher desorption temperature of the  
15 Unibeads 1S sample loop which can be heated faster and to a higher temperature without de-  
16 grading the material. Nevertheless, the residues on both adsorptive materials were on a tolera-  
17 ble level (below average measurement precision) for flask measurements with multiple meas-  
18 urements per sample.



## 1 4 Application

### 2 4.1 Laboratory operation: flask sample measurements

3 For quality assurance of the laboratory instrumentation, five air samples were analysed and  
4 compared to our reference GC-QPMS (gas chromatograph coupled to a quadrupole mass  
5 spectrometer) which uses a similar preconcentration setup (Hoker et al., 2015). Consistent  
6 results with the NOAA network (National Oceanic and Atmospheric Administration) were  
7 demonstrated for the GC-QPMS in the past during the IHALACE intercomparison (Hall et  
8 al., 2014), however with a different sample preconcentration using liquid nitrogen  
9 (Brinckmann et al., 2012; Laube and Engel, 2008; Laube et al., 2010). The current laboratory  
10 setup using the Stirling cooler-based preconcentration has been described by Hoker et al.  
11 (2015) and has shown very consistent results with previous measurements. The samples for  
12 the application and intercomparison discussed here were collected between July 7<sup>th</sup> and Sep-  
13 tember 11<sup>th</sup> 2015 at Mace Head Atmospheric Research Station in Ireland (53°20' °N,  
14 9°54' °W, 30 m above sea level). Samples were filled “moist” (no sample drying) into 2 L  
15 electro-polished stainless steel flasks (two flasks in parallel per sampling date). The compari-  
16 son is extended to include in-situ measurement data from the online monitoring Medusa  
17 GC-MS (Miller et al., 2008) operated by the AGAGE (Advanced Global Atmospheric Gases  
18 Experiment) network at Mace Head Station. Medusa GC-MS data points were chosen within  
19 ±1 hour of the flask samples’ sampling time. **Figure 6** shows a comparison of absolute quan-  
20 tification results for CFC-12 (CCl<sub>2</sub>F<sub>2</sub>). Very good agreement within the 1-fold measurement  
21 error is achieved in comparison to the Medusa GC-MS and within the 2-fold measurement  
22 error in comparison to the reference GC-QPMS. While the Medusa GC-MS is calibrated with  
23 secondary calibration gases (AGAGE flasks H-265 and H-266; CFC-12 scale: SIO-05), both  
24 our instruments were calibrated with different ternary calibration gasses, referenced to the  
25 same secondary calibration gas (AGAGE flask H-218; CFC-12 scale: SIO-05). Taking into  
26 account that all three instruments were calibrated with different calibration gases which rely  
27 on the same calibration scale but are based on a chain of intercalibrations, this result stands  
28 proof for highly accurate measurement results, excluding the absolute scale error.





## 1 4.2 Aircraft in-situ operation: GhOST-MS

2 Reliability of operation is best demonstrated with the in-situ GC-MS GhOST-MS<sup>1</sup>. **Figure 7**  
3 shows a chromatogram obtained from the injection of a pre-concentrated sample volume of  
4 100 mL of ambient air. With a chromatographic runtime of 2.9 minutes and a total cycle time  
5 of 4.1 minutes (see also **Table 1**), a data frequency is achieved that is very high for a GC-MS  
6 system with a total of 27 identified and simultaneously measured species on m/Q of bromine,  
7 chlorine and iodine in negative chemical ionisation mode using argon as reagent gas. The cy-  
8 cle time is limited by cooldown of the adsorptive material (HayeSep D) to  $-70\text{ }^{\circ}\text{C}$  needed to  
9 quantitatively trap the earliest eluting analyte, Halon 1301 (CBrF<sub>3</sub>). The very good overall  
10 performance of the GhOST-MS including the pre-concentration unit used in this in-situ appli-  
11 cation can be inferred from actual measurement data obtained during a research flight of the  
12 recent PGS campaign (POLSTRACC/GW-LCycle/SALSA) of the HALO aircraft on flight  
13 160226a (PGS-14). **Figure 8** shows a tracer-tracer correlation between Halon 1301 and Hal-  
14 on 1211 (CBrClF<sub>2</sub>). The measurements are colour-coded to show potential temperature  $\theta$ . As  
15 expected, the lowest mixing ratios are observed at the highest potential temperature. Both  
16 tracers have relatively long steady-state lifetimes of 72 years for Halon 1301 (58-97, derived  
17 from model data and observations) and 16 years for Halon 1211 (10-39, model data) (SPARC,  
18 2013) so that a compact correlation of mixing ratios of these two traces gases is expected in  
19 the stratosphere (Plumb and Ko, 1992). Due to its relatively low boiling point ( $-57.8\text{ }^{\circ}\text{C}$ ),  
20 Halon 1301 is the first species eluting from the chromatographic column. The shape of the  
21 chromatographic peak is thus strongly influenced by the injection, as refocusing on the chro-  
22 matographic column is expected to play a negligible role. As a correlation derived from  
23 measurement data can only be as compact as the measurement precision allows, the compact-  
24 ness of the correlation shown in **Figure 8** gives an indication of the high measurement preci-  
25 sion achieved with the GhOST-MS. The fact that this compact correlation includes a sub-  
26 stance whose precision is strongly influenced by its thermodesorption shows that the sample  
27 pre-concentration system on GhOST-MS is able to reproducibly trap and desorb even low boil-  
28 ing compounds like Halon 1301.

29 GhOST-MS has been deployed during a total of more than 200 flight hours on the HALO  
30 aircraft without a single failure of the pre-concentration unit. In addition, measurements with  
31 GhOST-MS were performed as part of the SHIVA campaign in Borneo, providing a complete  
32 bromine budget for the upper tropical troposphere up to about 13 km (Sala et al., 2014). The

<sup>1</sup> Manuscript on the current GhOST setup and characterisation in preparation by Keber et al.



- 1 preconcentration unit presented here therefore is not only able to provide high precision but is
- 2 also able to operate reliably under difficult conditions like aircraft operation with varying hu-
- 3 midity and temperatures, including operation during humid and hot conditions in the tropics.



## 1 **5 Summary and conclusion**

2 A single-stage, refrigerant-free sample preconcentration unit for ambient air analysis is pre-  
3 sented and characterised. The setup has proven to be applicable for both in-situ and laboratory  
4 operation and can quantitatively trap and desorb a wide range of halo- and hydrocarbons (see  
5 supplementary information). The use of different adsorptive materials is possible with the  
6 setup; two of which were used during this work, HayeSep D and Unibeads 1S. Both materials  
7 are well suited for analysis of halogenated trace gases in general. While HayeSep D is an es-  
8 tablished material for this task, Unibeads 1S potentially is a good alternative that has better  
9 heat tolerance and showed fewer sample loop blanks in the presented characterisation.

10 The preconcentration unit is positioned between more sophisticated but also more expensive  
11 and complicated solutions like e.g. the Medusa preconcentration unit described by Miller et  
12 al. (2008) and setups that use less powerful, Peltier-based cooling options that sacrifice ad-  
13 sorption temperature and therefore reduce the trappable substance range. The described setup  
14 is unique in terms of the used cooling technique, a Stirling cooler. The latter allows very low  
15 temperatures of  $-120\text{ }^{\circ}\text{C}$  tested in this work and  $-173\text{ }^{\circ}\text{C}$  reported by Eyer et al. (2016) for the  
16 preconcentration of methane with a comparable Stirling cooler without having to rely on a  
17 cooling agent like liquid nitrogen or liquid argon. The Stirling cooler as a cooling option is  
18 ideally suited for in-situ, remote-site operation, where refrigerant-based cooling options are  
19 very difficult to operate and space is limited – like the aircraft-based in-situ GC-MS instru-  
20 ment GhOST-MS. Moreover, the absence of mechanical/moving parts as well as the lack of  
21 necessity of vacuum insulation of cooled parts facilitates installation and maintenance. No  
22 exchange of adsorption tubes is necessary. Overall, the setup is relatively cheap with the Stir-  
23 ling cooler being the most expensive part by far.

24 The simplicity of the single-stage design also has a downside; a major problem is the trapping  
25 of large amounts of  $\text{CO}_2$  and injection into the detection system (see also section 3.2), espe-  
26 cially when using trapping temperatures below  $-80\text{ }^{\circ}\text{C}$ . Due to this limitation, the current con-  
27 figuration is not applicable to highly volatile compounds like  $\text{CF}_4$ ,  $\text{C}_2\text{F}_6$  or  $\text{C}_2\text{H}_6$ . Cooling ca-  
28 pacity should however be sufficient to ensure quantitative trapping of such compounds on a  
29 suitable adsorptive material. Therefore, a starting point for future improvement is removal of  
30  $\text{CO}_2$  to extend the already large substance range by compounds of higher volatility. Regarding  
31 desorption, no blank residues were found for halocarbons that would cause concern or render  
32 the setup unsuited for halocarbon analysis (see “Appendix B: Blank Residues”). However,



- 1 relatively large amounts of hydrocarbons remained in blank measurements. These blanks are
- 2 not an inherent problem of the preconcentration setup but more likely due to the adsorptive
- 3 materials used. Additional experiments are needed to reduce those uncertainties and extend
- 4 the applicability of the preconcentration unit to quantitative hydrocarbon analysis.



## 1 Acknowledgements

2 This work was supported by research grants of the Deutsche Forschungsgemeinschaft (DFG),  
3 EN367/12-1 (*FASTOF*), EN367/5-2 (*GhOST-MS*) and EN367/13-1 (*PGS*). We thank L. Mer-  
4 kel and the workshop of the institute for their contribution of technical drawings and compo-  
5 nent construction. Special thanks go to G. Spain for sample collection at Mace Head Station  
6 as well as the PGS campaign team lead by H. Oelhaf and B.-M. Sinnhuber which gave us the  
7 opportunity to create a set of excellent in-situ measurement data with the GhOST-MS.



## 1 **References**

- 2   Apel, E. C., Hills, A. J., Lueb, R. A., Zindel, S., Eisele, S., and Riemer, D. D.: A fast-GC/MS  
3   system to measure C<sub>2</sub> to C<sub>4</sub> carbonyls and methanol aboard aircraft, *J. Geophys. Res.*, 108,  
4   doi: 10.1029/2002jd003199, 2003.
- 5   Aragón, P., Atienza, J., and Climent, M. D.: Analysis of organic compounds in air: A review,  
6   *Crit. Rev. Anal. Chem.*, 30, 121-151, doi: 10.1080/10408340091164207, 2000.
- 7   Brinckmann, S., Engel, A., Bönisch, H., Quack, B., and Atlas, E.: Short-lived brominated  
8   hydrocarbons – observations in the source regions and the tropical tropopause layer, *Atmos.*  
9   *Chem. Phys.*, 12, 1213-1228, doi: 10.5194/acp-12-1213-2012, 2012.
- 10   de Blas, M., Navazo, M., Alonso, L., Durana, N., and Iza, J.: Automatic on-line monitoring of  
11   atmospheric volatile organic compounds: Gas chromatography-mass spectrometry and gas  
12   chromatography-flame ionization detection as complementary systems, *Sci. Total Environ.*,  
13   409, 5459-5469, doi: 10.1016/j.scitotenv.2011.08.072, 2011.
- 14   Demeestere, K., Dewulf, J., De Witte, B., and Van Langenhove, H.: Sample preparation for  
15   the analysis of volatile organic compounds in air and water matrices, *J Chromatogr A*, 1153,  
16   130-144, doi: 10.1016/j.chroma.2007.01.012, 2007.
- 17   Dettmer, K. and Engewald, W.: Ambient air analysis of volatile organic compounds using  
18   adsorptive enrichment, *Chromatographia*, 57, S339-S347, doi: 10.1007/BF02492126, 2003.
- 19   Eyer, S., Stadie, N. P., Borgschulte, A., Emmenegger, L., and Mohn, J.: Methane  
20   preconcentration by adsorption: A methodology for materials and conditions selection,  
21   *Adsorption*, 20, 657-666, doi: 10.1007/s10450-014-9609-9, 2014.
- 22   Eyer, S., Tuzson, B., Popa, M. E., van der Veen, C., Röckmann, T., Rothe, M., Brand, W. A.,  
23   Fisher, R., Lowry, D., Nisbet, E. G., Brennwald, M. S., Harris, E., Zellweger, C.,  
24   Emmenegger, L., Fischer, H., and Mohn, J.: Real-time analysis of δ<sup>13</sup>C- and δD-CH<sub>4</sub> in  
25   ambient air with laser spectroscopy: Method development and first intercomparison results,  
26   *Atmos. Meas. Tech.*, 9, 263-280, doi: 10.5194/amt-9-263-2016, 2016.
- 27   Farman, J. C., Gardiner, B. G., and Shanklin, J. D.: Large losses of total ozone in Antarctica  
28   reveal seasonal ClO<sub>x</sub>/NO<sub>x</sub> interaction, *Nature*, 315, 207-210, doi: 10.1038/315207a0, 1985.



- 1 Farwell, S. O., Gluck, S. J., Bamesberger, W. L., Schutte, T. M., and Adams, D. F.:  
2 Determination of sulfur-containing gases by a deactivated cryogenic enrichment and capillary  
3 gas chromatographic system, *Anal. Chem.*, 51, 609-615, doi: 10.1021/ac50042a007, 1979.
- 4 Haagen-Smit, A. J. and Fox, M. M.: Ozone formation in photochemical oxidation of organic  
5 substances, *Ind. Eng. Chem.*, 48, 1484-1487, doi: 10.1021ie51400a033, 1956.
- 6 Hall, B. D., Engel, A., Mühle, J., Elkins, J. W., Artuso, F., Atlas, E., Aydin, M., Blake, D.,  
7 Brunke, E. G., Chiavarini, S., Fraser, P. J., Happell, J., Krummel, P. B., Levin, I.,  
8 Loewenstein, M., Maione, M., Montzka, S. A., O'Doherty, S., Reimann, S., Rhoderick, G.,  
9 Saltzman, E. S., Scheel, H. E., Steele, L. P., Vollmer, M. K., Weiss, R. F., Worthy, D., and  
10 Yokouchi, Y.: Results from the international halocarbons in air comparison experiment  
11 (IHALACE), *Atmos. Meas. Tech.*, 7, 469-490, doi: 10.5194/amt-7-469-2014, 2014.
- 12 Helmig, D. and Greenberg, J. P.: Automated in situ gas chromatographic-mass spectrometric  
13 analysis of ppt level volatile organic trace gases using multistage solid-adsorbent trapping, *J.*  
14 *Chromatogr. A*, 677, 123-132, doi: 10.1016/0021-9673(94)80551-2, 1994.
- 15 Hodnebrog, Ø., Etminan, M., Fuglestedt, J. S., Marston, G., Myhre, G., Nielsen, C. J., Shine,  
16 K. P., and Wallington, T. J.: Global warming potentials and radiative efficiencies of  
17 halocarbons and related compounds: A comprehensive review, *Rev. Geophys.*, 51, 300-378,  
18 doi: 10.1002/rog.20013, 2013.
- 19 Hoker, J., Obersteiner, F., Bönisch, H., and Engel, A.: Comparison of GC/time-of-flight MS  
20 with GC/quadrupole MS for halocarbon trace gas analysis, *Atmos. Meas. Tech.*, 8, 2195-  
21 2206, doi: 10.5194/amt-8-2195-2015, 2015.
- 22 Hou, Y., Yang, L., Wang, B., Xu, J., Yang, Y., Yang, Y., Cao, Q., and Xie, X.: Analysis of  
23 chemical components in tobacco flavors using stir bar sorptive extraction and thermal  
24 desorption coupled with gas chromatography-mass spectrometry, *Chinese Journal of*  
25 *Chromatography*, 24, 601-605, doi: 10.1016/S1872-2059(06)60026-6, 2006.
- 26 Laube, J. C. and Engel, A.: First atmospheric observations of three chlorofluorocarbons,  
27 *Atmos. Chem. Phys.*, 8, 2008.
- 28 Laube, J. C., Kaiser, J., Sturges, W. T., Bönisch, H., and Engel, A.: Chlorine isotope  
29 fractionation in the stratosphere, *Science*, 329, 1167, doi: 10.1126/science.1191809, 2010.



- 1 Marengo, A., Gouget, H., Nédélec, P., Pagés, J.-P., and Karcher, F.: Evidence of a long-term  
2 increase in tropospheric ozone from Pic Du Midi data series: Consequences: Positive radiative  
3 forcing, *J. Geophys. Res.-Atmos.*, 99, 16617-16632, doi: 10.1029/94JD00021, 1994.
- 4 Miller, B. R., Weiss, R. F., Salameh, P. K., Tanhua, T., Grealley, B. R., Mühle, J., and  
5 Simmonds, P. G.: Medusa: A sample preconcentration and GC/MS detector system for in situ  
6 measurements of atmospheric trace halocarbons, hydrocarbons, and sulfur compounds, *Anal.*  
7 *Chem.*, 80, 1536-1545, doi: 10.1021/ac702084k, 2008.
- 8 Molina, M. J. and Rowland, F. S.: Stratospheric sink for chlorofluoromethanes: Chlorine atom  
9 catalysed destruction of ozone, *Nature*, 249, 810-812, doi: 10.1038/249810a0, 1974.
- 10 Monks, P. S., Archibald, A. T., Colette, A., Cooper, O., Coyle, M., Derwent, R., Fowler, D.,  
11 Granier, C., Law, K. S., Mills, G. E., Stevenson, D. S., Tarasova, O., Thouret, V., von  
12 Schneidemesser, E., Sommariva, R., Wild, O., and Williams, M. L.: Tropospheric ozone and  
13 its precursors from the urban to the global scale from air quality to short-lived climate forcer,  
14 *Atmos. Chem. Phys.*, 15, 8889-8973, doi: 10.5194/acp-15-8889-2015, 2015.
- 15 Montzka, S. A., Reimann, S. (Coordinating Lead Authors), Engel, A., Krüger, K., O'Doherty,  
16 S., Sturges, W. T. L. A., Blake, D., Dorf, M., Fraser, P., Froidevaux, L., Jucks, K., Kreher, K.,  
17 Kurylo, M. J., Mellouki, A., Miller, J., Nielsen, O.-J., Orkin, V. L., Prinn, R. G., Rhew, R.,  
18 Santee, M. L., Stohl, A., and Verdonik, D. C.: Ozone-depleting substances (ODSs) and related  
19 chemicals. Chapter 1 in: Scientific assessment of ozone depletion: 2010, global ozone  
20 research and monitoring project report no. 52., World Meteorological Organization (WMO),  
21 Geneva, Switzerland, 108 pp., 2011.
- 22 O'Doherty, S. J., Simmonds, P. G., and Nickless, G.: Analysis of replacement  
23 chlorofluorocarbons using carboxen microtraps for isolation and preconcentration in gas  
24 chromatography-mass spectrometry, *J. Chromatogr. A*, 657, 123-129, doi: 10.1016/0021-  
25 9673(93)83043-r, 1993.
- 26 Obersteiner, F., Bönisch, H., and Engel, A.: An automated gas chromatography time-of-flight  
27 mass spectrometry instrument for the quantitative analysis of halocarbons in air, *Atmos.*  
28 *Meas. Tech.*, 9, 179-194, doi: 10.5194/amt-9-179-2016, 2016.





- 1 Plumb, R. A. and Ko, M. K. W.: Interrelationships between mixing ratios of long-lived  
2 stratospheric constituents, *Journal of Geophysical Research: Atmospheres*, 97, 10145-10156,  
3 doi: 10.1029/92jd00450, 1992.
- 4 Saito, T., Yokouchi, Y., Stohl, A., Taguchi, S., and Mukai, H.: Large emissions of  
5 perfluorocarbons in east asia deduced from continuous atmospheric measurements, *Environ.*  
6 *Sci. Technol.*, 44, 4089-4095, doi: 10.1021/es1001488, 2010.
- 7 Sala, S., Bönisch, H., Keber, T., Oram, D. E., Mills, G., and Engel, A.: Deriving an  
8 atmospheric budget of total organic bromine using airborne in situ measurements from the  
9 western pacific area during SHIVA, *Atmos. Chem. Phys.*, 14, 6903-6923, doi: 10.5194/acp-  
10 14-6903-2014, 2014.
- 11 Simmonds, P. G., O'Doherty, S., Nickless, G., Sturrock, G. A., Swaby, R., Knight, P.,  
12 Ricketts, J., Woffendin, G., and Smith, R.: Automated gas chromatograph/mass spectrometer  
13 for routine atmospheric field measurements of the CFC replacement compounds, the  
14 hydrofluorocarbons and hydrochlorofluorocarbons, *Anal. Chem.*, 67, 717-723, doi:  
15 10.1021/ac00100a005, 1995.
- 16 Solomon, S.: Stratospheric ozone depletion: A review of concepts and history, *Rev. Geophys.*,  
17 37, 275, doi: 10.1029/1999rg900008, 1999.
- 18 Song, C.-F., Kitamura, Y., Li, S.-H., and Ogasawara, K.: Design of a cryogenic CO<sub>2</sub> capture  
19 system based on stirling coolers, *International Journal of Greenhouse Gas Control*, 7, 107-  
20 114, doi: 10.1016/j.ijggc.2012.01.004, 2012.
- 21 SPARC: Sparc report on the lifetimes of stratospheric ozone-depleting substances, their  
22 replacements, and related species, M. Ko, P. Newman, S. Reimann, S. Strahan (Eds.), SPARC  
23 Report No. 6, WCRP-15/2013, 2013.
- 24 Velders, G. J., Fahey, D. W., Daniel, J. S., McFarland, M., and Andersen, S. O.: The large  
25 contribution of projected HFC emissions to future climate forcing, *Proc. Natl. Acad. Sci. U. S.*  
26 *A.*, 106, 10949-10954, doi: 10.1073/pnas.0902817106, 2009.

27



## 1 Tables

2 **Table 1.** Cycle times at  $T_A$  of  $-80\text{ °C}$  /  $-120\text{ °C}$  (laboratory setup) and  $-70\text{ °C}$  (in-situ setup), based on  
 3 operational data. Laboratory setup configuration: Sunpower CryoTel CT Stirling cooler, preconcentra-  
 4 tion volume:  $500\text{ mL}$  at  $100\text{ mL}\cdot\text{min}^{-1}$ ,  $T_D \approx 200\text{ °C}$  for 3 min. In-situ setup configuration: Twinbird  
 5 SC-TD08 Stirling cooler, preconcentration volume:  $100\text{ mL}$  at  $100\text{ mL}\cdot\text{min}^{-1}$ ,  $T_D \approx 200\text{ °C}$  for 1 min.  
 6 Adsorptive material, both setups: HayeSep D. Due to a smaller coldhead, cooling rate and warm-up  
 7 during desorption are considerably larger with the in-situ setup, despite the shorter desorption time.

$T_A$ [°C]	cooling rate at $T_A$ [°C·min <sup>-1</sup> ]	warm-up during desorption [°C]	minimum cycle time including preconcentration after $T_A$ is reached [min]
Laboratory instrument (GC-TOFMS)			
-80	-2.2	7.7	8.5
-120	-1.2	16.3	18.6
In-situ instrument (GhOST-MS)			
-70	-4.1	13.5	4.1

8



1 **Table 2.** Results from a volume variation experiment, comprising measurements of the same reference  
 2 air with preconcentration volumes (PrcVol) of up to 2, 5 and 10 L. Laboratory setup, adsorptive mate-  
 3 rial Unibeads 1S. Volume-corrected detector response is referenced against calibration preconcentra-  
 4 tion volumes of 1 L (rR). rR <100% indicates underestimation (e.g. loss by breakthrough); rR >100%  
 5 indicates overestimation (e.g. increase by a memory effect from the preceding sample or contamina-  
 6 tion). Breakthrough is observed for COS at a preconcentration volume of 10 L while ethyne shows  
 7 signs of a system contamination (rR >100% despite a higher volatility compared to COS). CFC-12 and  
 8 CFC-11 show no indication of breakthrough, with all deviations from 100% rR below 3  $\sigma$ .

Substance	PrcVol [L]	rR	rR: 1 $\sigma$	PrcVol [L]	rR	rR: 1 $\sigma$	PrcVol [L]	rR	rR: 1 $\sigma$
Ethyne (C <sub>2</sub> H <sub>2</sub> )	2	102.0%	0.66%	5	108.9%	0.70%	10	109.2%	0.70%
Carbonyl sulfide (COS)		102.2%	0.82%		100.9%	0.81%		64.8%	0.52%
CFC-12 (CCl <sub>2</sub> F <sub>2</sub> )		99.9%	0.41%		100.7%	0.42%		100.6%	0.42%
CFC-11 (CCl <sub>3</sub> F)		100.2%	0.21%		100.5%	0.22%		100.6%	0.22%

9



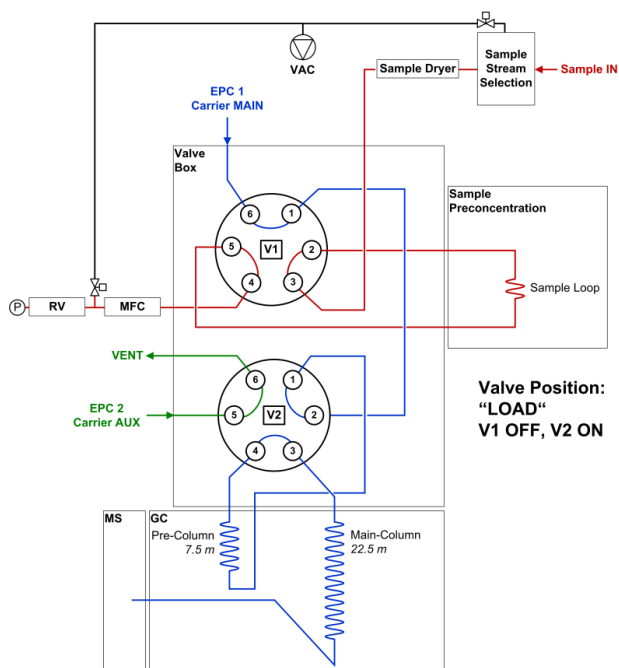
1 **Table 3.** Retention times  $t_R$  with relative standard deviations rSD and variances in [s] for selected sub-  
 2 stances (same as **Table 2**) as well as their respective average signal width expressed as FWHM in [s].  
 3 Values derived from 112 individual measurements of different ambient air samples using the ramped  
 4 GC program. Sample loop adsorptive material: HayeSep D. HFC-23 is the first detectable substance,  
 5 least separated by chromatography. CFC-11 can be considered a reference for optimal chromatograph-  
 6 ic performance of the given setup.

Substance	$t_R$ [min]	$t_R$ rSD	Variance [s]	Avg. Peak Width [s]
HFC-23 (CHF <sub>3</sub> )	3.01	0.105%	0.0386	4.09
Ethyne (C <sub>2</sub> H <sub>2</sub> )	3.74	0.047%	0.0118	2.77
Carbonyl sulfide (COS)	3.86	0.040%	0.0092	2.29
CFC-12 (CCl <sub>2</sub> F <sub>2</sub> )	5.01	0.014%	0.0018	2.26
CFC-11 (CCl <sub>3</sub> F)	7.25	0.006%	0.0008	2.24

7

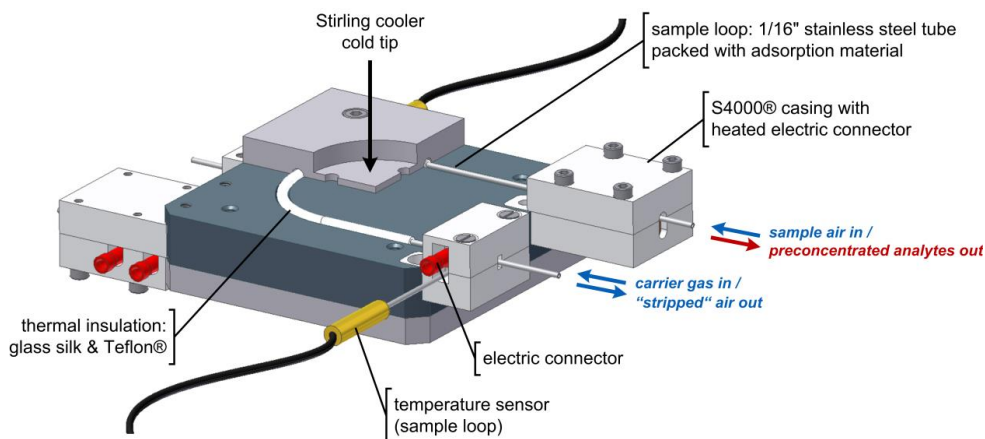


## 1 Figures



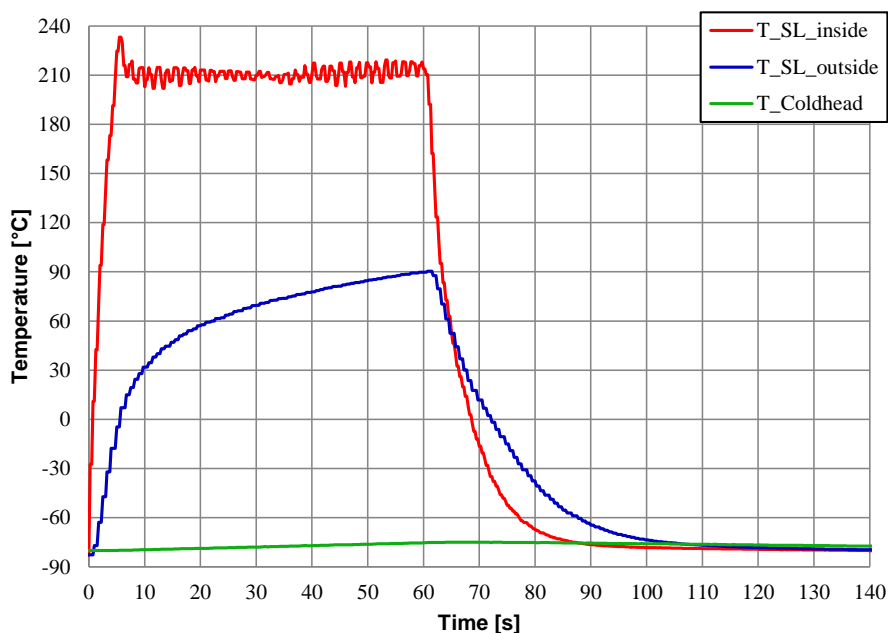
2

3 **Figure 1.** Flow scheme showing the gas flow during pre-concentration. Two electronic pressure  
4 controllers, EPC 1 and EPC 2, control the carrier gas flow. The two 6-port 2-position rotary  
5 valves V1 and V2 are set to OFF/ON position. A sample is pre-concentrated (red flow path);  
6 sample components not trapped in the sample loop flow through the mass flow controller  
7 (MFC) into the reference volume (RV). By switching V1 to ON position (for desorption), the  
8 sample loop is injected onto the GC column. Sample loop as well as reference volume and  
9 stream selection valves are evacuated prior to the pre-concentration of the next sample. By  
10 switching V2 to OFF, it separates pre- and main-column; the pre-column is flushed backwards.  
11 This prevents high-boiling, non-targeted species from reaching the main-column.



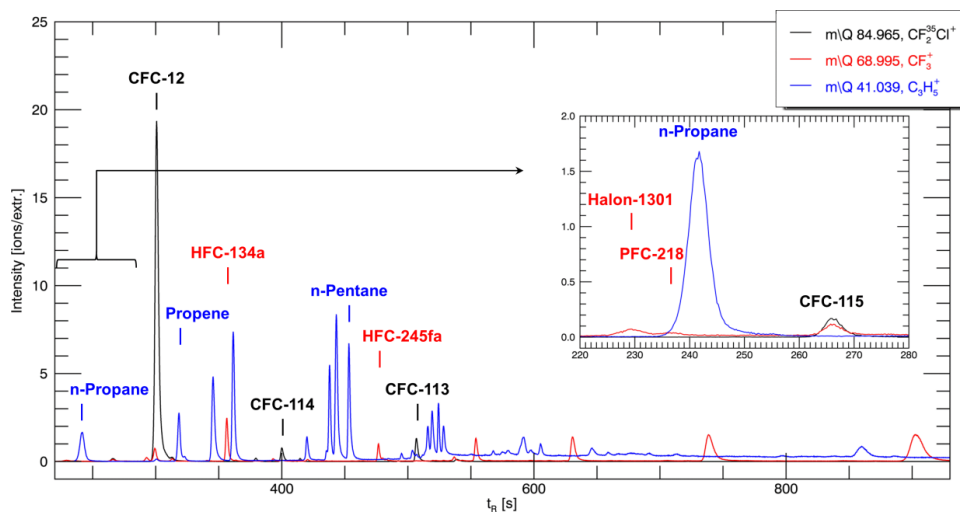
1

2 **Figure 2.** Technical drawing of the coldhead and sample loop placed inside. Three plates of  
3 anodized aluminium can hold two sample loops. The Stirling cooler's cold tip screwed to the  
4 coldhead removes heat for cooling. Heat for sample desorption is generated by a current directly  
5 applied to the sample loop. The electric connector in the direction of sample flow (upper right  
6 side of the drawing) is heated constantly to 150 °C to avoid a cold point due to the mass of the  
7 electric connector and its proximity to the coldhead (S4000® insulation material:  
8 Brandenburger, Germany).



1

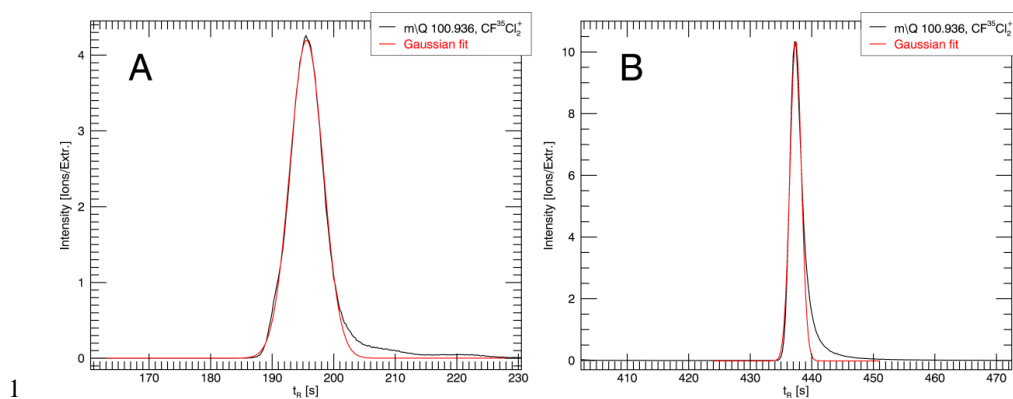
2 **Figure 3.** Desorption temperature curve inside the sample loop with a preceding adsorption  
3 temperature of  $-80\text{ }^{\circ}\text{C}$  and a subsequent cool-down from desorption to adsorption temperature.  
4 Red curve, “T\_SL\_inside”: signal from temperature sensor shifted inside the sample loop. Blue  
5 curve, “T\_SL\_outside”: temperature sensor signal from the sensor welded to the outer sample  
6 loop tubing wall. Green curve, “T\_Coldhead”: temperature of the coldhead. Deterministic  
7 heater, output in this example: 50 % in stage 1, held 5 s, and 30 % in stage 2, held 55 s. The  
8 periodic oscillation of  $T_D$  observed is a result of a very slow pulse width modulation used in the  
9 testing setup: 100 ms period with 10 ms minimum increment.



1

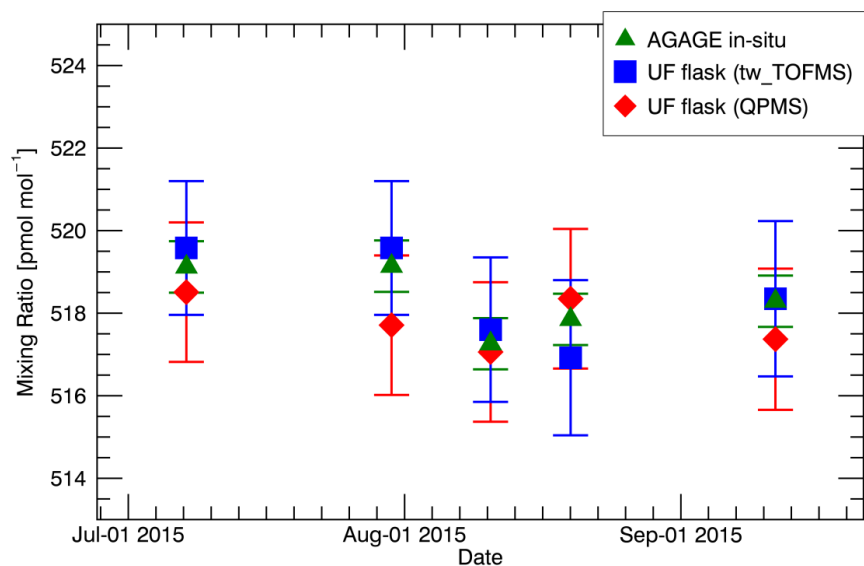
2 **Figure 4.** Chromatogram from a 1 L ambient air sample obtained with the GC-MS setup  
3 described in Obersteiner et al., 2016. X-axis: retention time  $t_R$  in seconds. Y-axis: signal  
4 intensity expressed as ions per extraction which are derived from a 22.7 kHz TOFMS extraction  
5 rate, averaged to yield a mass spectra rate of 4 Hz. X- and Y-axis description also valid for the  
6 magnified section. Black graph: mass-to-charge ratio ( $m/Q$ ) = 84.965 signal from a typical CFC  
7 fragment ion  $CF_2^{35}Cl^+$ . Red graph:  $m/Q$  = 68.995 signal from a typical PFC or HFC fragment  
8 ion  $CF_3^+$ . Blue graph:  $m/Q$  = 41.039 signal from a typical hydrocarbon fragment ion  $C_3H_5^+$ . The  
9 magnified section shows the chromatographic peak of n-propane and three other compounds to  
10 demonstrate injection quality of substances least re-focused by chromatography.





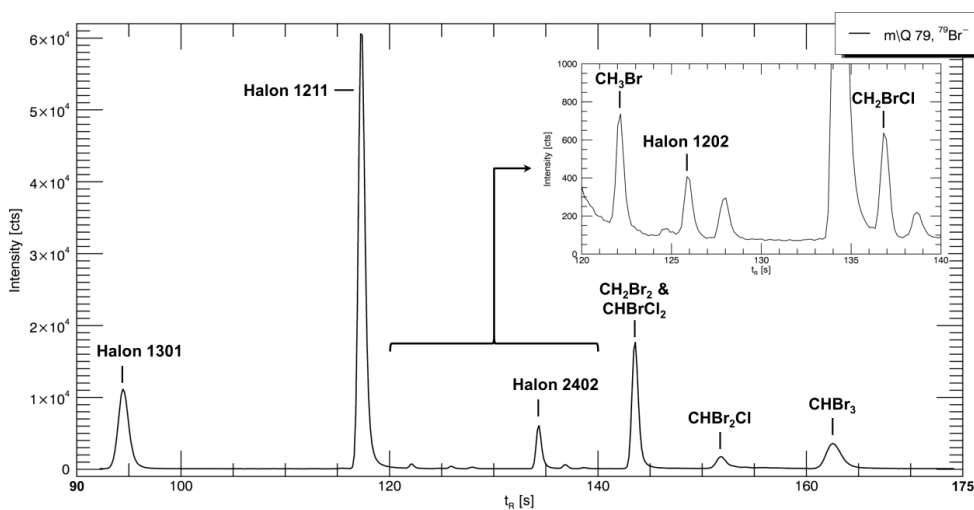
1

2 **Figure 5.** Comparison of chromatographic peak shapes of the  $\text{CF}^{35}\text{Cl}_2^+$  fragment ion signal of  
3 CFC-11 ( $\text{CFCl}_3$ ), from an injection of 1 L pre-concentrated ambient air onto the GC column kept  
4 isothermal at 150 °C (A) and onto the GC column kept at 45 °C and ramped to 200 °C  
5 subsequently (B) (see section 3.1). X-axis: retention time  $t_R$  in seconds;  $t_R$  interval shown is 70 s  
6 in both plots. Y-axis: signal intensity expressed as ions per extraction (see **Figure 4**). The red  
7 curve shows a Gaussian fit for comparison of actual peak shape and a peak shape that is  
8 considered ideal. FWHM of fit: (A) 6.3 s (0.10 min) and (B) 2.0 s (0.03 min). Adsorptive  
9 material: Unibeads 1S.



1

2 **Figure 6.** CFC-12 ( $\text{CCl}_2\text{F}_2$ ) mixing ratios at Mace Head Atmospheric Research Station, Ireland  
3 ( $53^\circ 20' \text{N}$ ,  $9^\circ 54' \text{W}$ , 30 m above sea level) derived from 2 L stainless steel flask samples  
4 measured with the instrument in description (GC-TOFMS, blue squares), our reference  
5 instrument (GC-QPMS, red diamonds) and values taken from the online measurement data of  
6 the in-situ Medusa GC-MS (green triangles). Error bars: 1-fold measurement precision of each  
7 instrument (Medusa system: typical precision taken from Miller et al. (2008)). Calibration scale,  
8 all instruments: SIO-05.



1

2

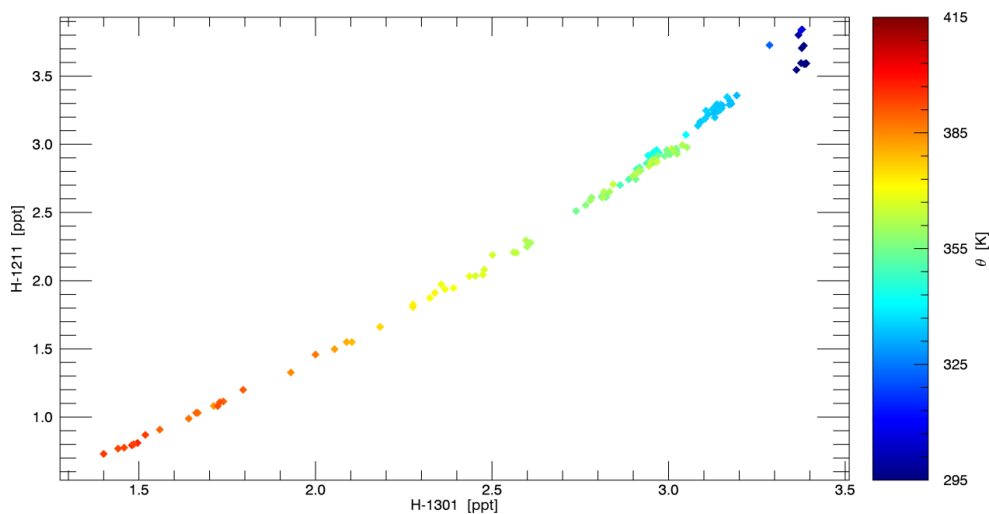
3

4

5

6

**Figure 7.** Chromatogram from a preconcentration of 0.1 L ambient air obtained with the in-situ GC-MS setup GhOST-MS. X-axis: retention time  $t_R$  in seconds. Y-axis: signal intensity in counts, arbitrary unit. MS: Agilent 5975C in negative chemical ionization mode (reagent: argon). Black graph: mass-to-charge ratio  $m/Q = 79$  signal of  $^{79}\text{Br}^-$  ions from brominated trace gases.



1

2 **Figure 8.** Tracer-tracer correlation of Halon 1301 ( $\text{CBrF}_3$ , x-axis) vs. Halon 1211 ( $\text{CBrClF}_2$ ,  
3 y-axis). Color code indicates potential temperature  $\theta$  in [K]. Data was obtained during the  
4 POLSTRACC mission with the HALO aircraft, flight 160226a (PGS-14). Preliminary data;  
5 calibration scale of Halon 1301 and 1211: SIO-05.